

Evaluation of antioxidant treatments for the modulation of macrophage function in the context of retinal degeneration

Sarah Elbaz-Hayoun, Batya Rinsky, Shira Hagbi-Levi, Michelle Grunin, Tammy Haya Yedid, Itay Chowers

Department of Ophthalmology, Hadassah-Hebrew University Medical Center, and the Hebrew University – Hadassah School of Medicine

Purpose: Oxidative stress and macrophages have been implicated in the pathogenesis of atrophic and neovascular age-related macular degeneration (aAMD and nvAMD). It is unclear whether oxidative injury mediates macrophage involvement in AMD. We aimed to investigate the effect of antioxidant treatments on human monocyte-derived macrophages (hMDMs) from patients with AMD in models for the disease.

Methods: Four antioxidant treatments were evaluated (G1: lutein + zeaxanthin, G2: lutein + zeaxanthin and zinc, G3: lutein + zeaxanthin, zinc, Lyc-O-Mato, and carnosic acid, G4: lutein + zeaxanthin, carnosic acid, and beta-carotene, G5: olive oil as vehicle control). The compounds were added to the culture medium of M1 (interferon-gamma [IFN- γ] and lipopolysaccharide [LPS]) and M2a (interleukin-13 [IL-13] and IL-4) hMDMs from patients with AMD (n=7 and n=8, respectively). Mouse choroidal tissue was cultured with supernatants from treated M1/M2a hMDMs, to evaluate the effect of treatments on the angiogenic properties of macrophages with choroidal sprouting assay (CSA). Mouse retinal explants were cultured with treated hMDMs for 18 h, and evaluated for photoreceptor apoptosis using terminal deoxynucleotidyl transferase dUTP nick end labeling (TUNEL) labeling. Adult BALB/c mice (n=8) were exposed to 8,000 lux bright light for 3 h, and treated orally with antioxidant supplements for 7 days that preceded light injury and following it. Oxidative stress was assessed using an anti-4-hydroxynonenal (4-HNE) antibody. Retinal function and the thickness of the outer nuclear layer were evaluated with electroretinography (ERG) and histological analysis, respectively.

Results: The G3 treatment reduced M2a hMDMs-associated sprouting in the CSA compared to the untreated group (n=7, -1.52-fold, p=0.05). Conversely, the G2 treatment was associated with an increased neurotoxic effect of M2a hMDMs in the retinal explant assay compared to the control group (n=7, 1.37-fold, p=0.047), as well as compared to the G3 treatment group (1.46-fold, p=0.01). The G4 treatment was also associated with increased cytotoxicity compared to the control group (1.48-fold, p=0.004), and compared to the G3 treatment group (1.58-fold, p=0.001). In the in vivo light damage model, mice (n=8) supplemented with G2, G3, and G4 had decreased levels of oxidative injury assessed using 4-HNE labeling (-2.32-fold, -2.17-fold, and -2.18-fold, respectively, p<0.05 for all comparisons). None of the treatments were associated with reduced photoreceptor cell loss, as shown with histology and ERG.

Conclusions: Antioxidant treatment modulates M2a hMDMs at the functional level. In particular, we found that the G3 combination has a beneficial effect on M2a macrophages in reducing their angiogenic and neurotoxic capacity ex vivo. In addition, antioxidant treatments considerably reduced the oxidative stress level in light-damaged retinas. Further research is required to assess whether such therapies may curb macrophage-driven photoreceptor loss and neovascularization in AMD.

Recent studies have provided additional support for the involvement of immune cells, particularly monocytes and their macrophage descendants, in the pathogenesis of age-related macular degeneration (AMD). The presence of macrophages in the vicinity of AMD lesions [1,2], and the increased level of monocyte chemokine attractant (MCP-1) in the aqueous humor of patients with AMD [3], together with increased expression of its receptor (CCR2), in a subclass of the monocytes of patients with AMD, and the proinflammatory gene expression signature in monocytes from patients with AMD [4] implicate these cells in the disease.

Different subtypes of macrophages exist, among them M1 and M2 polarized macrophages. These subtypes represent the two extremes in the polarization spectrum of macrophages [5,6]. M1 macrophages are generally known as proinflammatory macrophages [7,8], whereas M2a macrophages are often associated with tissue remodeling and repair [9,10]. Nevertheless, the distinct roles of the two subtypes in the context of AMD are elusive. Subtypes of macrophages may have specific functions in the context of AMD. For example, we previously found a proangiogenic effect of M1 human monocyte-derived macrophages (hMDMs) from patients with AMD on choroidal sprouting assay (CSA), and in the laser-induced choroidal neovascularization (LI-CNV) model in rats [11], while others found that CCR2+ monocytes

Correspondence to: Itay Chowers, Department of Ophthalmology, Hadassah-Hebrew University Medical Center, POB 12000, Jerusalem, Israel 91120; Phone: +972-2-6777228; FAX: +972-2-6777228; email: chowers@hadassah.org.il

induce photoreceptor degeneration in experimental subretinal inflammation in Cx3cr1^{-/-}-deficient mice [12].

An important mechanism that may partially underlie the involvement of macrophages in AMD is their capability to generate reactive oxygen species (ROS) [13], because oxidative injury represents one of the hallmarks of this disease [14]. ROS in the eye can accelerate photoreceptor and RPE cell death, as well as increase the inflammation and angiogenesis level [15-17]. Accordingly, oral supplements of antioxidant vitamins and minerals are the only current validated treatment that reduces the prevalence of progression from atrophic AMD (aAMD) to the neovascular form of the disease (nvAMD) [18].

We previously found that several antioxidant formulas exert a beneficial effect on macrophage cells, in terms of modulating antioxidant and proinflammatory gene and protein expression [19]. In the present study, we evaluated the effect of antioxidant supplement combinations on the modulation of hMDM function, and on the preservation of photoreceptors, in *in vitro* and *in vivo* models that recapitulate features of AMD.

METHODS

Monocyte isolation and hMDM polarization: Monocyte/hMDM culture was performed as previously described [11]. Patients with nvAMD (n=8, five women, three men, mean age ± standard error of the mean [SEM]: 77.4±4.7 years, range: 66–92) were recruited from the retina clinic of the Department of Ophthalmology at the Hadassah-Hebrew University Medical Center. Criteria for inclusion of patients with nvAMD included age over 55 years, diagnosis of AMD according to the Age-Related Eye Disease Study Research Group (ARED) [20] criteria, and diagnosis of CNV according to fluorescein angiogram and optical coherence tomography. Eyes with neovascular lesions that comprised less than 50% active CNV, subretinal hemorrhage greater than 25% of the lesion size, or the presence of other retinal diseases were excluded from the study. Specifically, eyes with any other potential cause of CNV, such as myopia, trauma, or uveitis, were excluded. Also excluded were patients with a major systemic illness, such as cancer, autoimmune disease, congestive heart failure, or uncontrolled diabetes. All patients signed an informed consent form, and the study was approved by the institutional ethics committee (see the Ethics Declaration). Blood samples (30 ml) were collected from patients with nvAMD in EDTA tubes (BD Bioscience, Franklin Lakes, NJ). Monocytes were isolated from whole blood, differentiated, and activated into M1 (interferon- γ [IFN- γ] and lipopolysaccharide [LPS]) and M2a

(interleukin-4 [IL-4] and IL-13) phenotypes (M1 and M2a hMDMs, respectively), as previously described [5,21-24]. Briefly, peripheral blood mononuclear cells (PBMCs) were separated using a Histopaque-Ficoll density centrifuge according to the manufacturer's recommendations (Sigma-Aldrich, Munich, Germany). PBMCs (3×10^7 cells/cm²) were suspended in RPMI 1640 medium (Biologic Industries Israel Beit Haemek Ltd, Kibbutz Beit Haemek, Israel), and seeded into six-well plates coated with the amino acid poly-D-lysine, which facilitates the adherence of monocytes. Two hours after incubation in a 37 °C and 5% CO₂ cell culture incubator, the cells were washed with PBS (1X; 120 mM NaCl, 20 mM KCl, 10 mM NaPO₄, 5 mM KPO₄, pH 7.4), and monocytes were cultured for 7 days in RPMI 1640 supplemented with 10% fetal calf serum (FCS), 1% nonessential amino acid, 2 mmol/l L-glutamine, 1 mM sodium pyruvate, 100 units/ml penicillin and 100 µg/ml streptomycin, and 50 ng/ml macrophage colony-stimulating factor (M-CSF, PeproTech, Rocky Hill, NJ). M-CSF was added to the growth medium to induce maturation of the monocytes to hMDMs. Polarization of hMDMs to the M1 (IFN- γ and LPS) phenotype was obtained with the addition of 20 ng/ml IFN- γ (PeproTech) and 100 ng/ml LPS (Sigma-Aldrich) at day 6. To obtain the M2a (IL-4 and IL-13) phenotype, 50 ng/ml IL-13 (PeproTech) and 20 ng/ml IL-4 (PeproTech) were added at day 5 of culture. As M1 (IFN- γ and LPS) macrophages require 24 h for polarization whereas M2a (IL-4 and IL-13) macrophages need 48 h [25], the hMDMs were polarized on different days, so that *in vitro* experiments would be performed on the same day. The hMDMs were collected with 0.025% trypsin (TRI Reagent; Sigma-Aldrich) which was deactivated with RPMI + FCS, following three washes with PBS to remove traces of supernatant, so that pure cells remained.

Supplement composition and administration: Four different formulas were tested based on our previous research [19]. The ingredients were diluted in olive oil. For the *in vivo* studies, five groups of mice were treated with the four different formulas and a control group of olive oil, with gavage, during the 7 days that preceded the light injury and 7 days following it. The formula compositions were as follows: G1: lutein + zeaxanthin (Katra, Karnataka, India; 75 mg/kg); G2: lutein + zeaxanthin (75 mg/kg) and zinc (1.44 mg/kg; Navkar, Maharashtra, India); G3: lutein + zeaxanthin (75 mg/kg), zinc (1.44 mg/kg), Lyc-O-Mato (100 mg/kg; standardized tomato extract containing lycopene [6%], as well as other tomato phytonutrients, like phytoene, phytofluene, tocopherols, and phytosterols; Lycored, Be'er Sheva, Israel), and carnosic acid (100 mg/kg; added as rosemary extract containing 20% CA; Lycored); G4: lutein + zeaxanthin (75 mg/kg), carnosic acid (100 mg/kg), and beta-carotene (100 mg/kg); and G5: olive oil

as vehicle control. For the ex vivo retinal explant and choroid sprouting assays, supplements were added to the culture media at the time of induction of macrophage polarization. The concentrations of the different compounds in culture were chosen to mimic serum levels obtained following oral supplementation as follows: G1: lutein + zeaxanthin (1 μ M; 0.2 μ M); G2: lutein + zeaxanthin (1 μ M; 0.2 μ M) and zinc (10 μ M); G3: lutein + zeaxanthin (1 μ M; 0.2 μ M), zinc (10 μ M), Lyc-O-Mato (2 μ M), and carnosic acid (2 μ M); G4: lutein + zeaxanthin (1 μ M; 0.2 μ M), carnosic acid (2 μ M), and beta-carotene (2 μ M), and G5: vehicle control.

Choroid sprouting assay: An ex vivo angiogenesis assay was performed to evaluate the effect of the different antioxidant treatments on the supernatant of M1 (IFN- γ and LPS)/M2a (IL-4 and IL-13) hMDMs as previously described [26]. Briefly, the supernatant of the two types of polarized hMDMs was collected and kept in -20°C until used. C57bl/6 4- to 6-week-old mice (n=7) that were treated in accordance with the guidelines of the Association for Research in Vision and Ophthalmology (ARVO) were used. Experiments were conducted with the approval of the institutional animal care ethics committee. Five minutes after ketamine was injected, the animals were checked for responses, and euthanized with cervical dislocation. The eyes were immediately enucleated and kept in ice-cold CO_2 -independent medium (cat. 18045-054; Gibco, Paisley, Scotland) containing 100 units/ml penicillin-streptomycin and 1% glutamine before dissection. A choroid-sclera complex from the mice was gently dissected along with the RPE. The complex was cut into 1-mm pieces. Fragments were embedded in 30 μ l of growth factor-reduced Matrigel (BD Biosciences, Cat. 354,230) in 24-well plates. The thickness of the Matrigel was approximately 0.4 mm. The plates were then incubated for 10 min in 37°C , in a 5% CO_2 cell culture incubator without medium to solidify the Matrigel. A mix of 250 μ l of medium containing endothelial cell growth medium (ECGM; C-22010, PromoCell, Heidelberg, Germany), 2.5% supplement mix (C-9215, PromoCell), 5% FCS, 100 units/ml penicillin-streptomycin and 1% glutamine, and 250 μ l of the hMDM culture supernatant was added to each well. Medium for each well was changed every 3 days. and the cultures were fixed with 4% paraformaldehyde after 8 days. The cultures were viewed with an inverted phase-contrast CKX41 Olympus microscope, and images were photographed with an Olympus DP70 digital camera (Olympus, Tokyo, Japan). ImageJ software was used to quantify the sprouting area. The scale was set to convert pixels to square millimeters. Each picture was converted to 8-bit type to obtain a binary image. The sprouting area was then selected, and measured after the choroid tissue was excluded.

Macrophage coculture with mouse retinal explants: C57bl/6 mouse retinas (n=7) were dissected and incubated with polarized hMDMs (n=7) which were exposed to the different treatments as previously described [12]. Briefly, the different groups of treated hMDMs were harvested, and seeded for a minimum of 2 h on polycarbonate filter into serum-free Dulbecco's Modified Eagle Medium (DMEM; Biologic Industries, Kibbutz Beit Haemek, Israel) medium supplemented with glutamine and penicillin-streptomycin. In parallel, the C57bl/6 mice were anesthetized and then euthanized with cervical dislocation. The eyes were enucleated, and kept in cold serum-free DMEM medium supplemented with glutamine and penicillin-streptomycin. The retinas were gently detached from the choroid tissue, and they were immediately placed on the polycarbonate filter so that hMDMs were in contact with the photoreceptors layer. After 18 h of incubation, the mouse retinas were fixed with methanol, and terminal deoxynucleotidyl transferase dUTP nick end labeling (TUNEL) labeling was performed according to the manufacturer's instructions (In Situ Cell Death Detection Kit, TMR red, La Roche, Basel, Switzerland). A Zeiss LSM710 confocal laser scanning system (Carl Zeiss MicroImaging GmbH, Jena, Germany) was used to visualize the stained cells, and ImageJ was used to perform automatic quantification of the cells.

Model of photic retinal injury: Albino (BALB/c) mice underwent genotyping to validate homozygosity to the wild-type *crbl*, *gnat2*, and *rpe65* genes [27-29]. The process of photic injury was established according to the standard protocol [30], and optimized to validate an approximately 50% reduction in thickness of the outer nuclear layer. Briefly, after 1 h of dark adaptation, 6-week-old albino mice (n=8) that were raised under a normal 12 h:12 h light-dark cycle were exposed to 8,000 lux of white light of fluorescence tubes for a period of 3 h. Light damage was performed according to the appropriate circadian rhythm time period: dilation with Cyclogyl (one drop per eye, Farmaceutica, S.A, Madrid, Spain) and 5% phenylephrine (Fischer Pharmaceutical Labs, Bnei Brak, Israel) at 9:30 AM under red light and the light-level adjustment at 9:45 AM. Light damage was performed between 10 AM and 1 PM. During the light damage, the mice were placed into a cage (maximum two mice per cage) lined with aluminum foil, and temperature under 30°C was maintained. Immediately after light damage, the mice were returned to the normal 12 h:12 h light-dark cycle.

Electroretinography recording: Full-field electroretinography (ERG) was performed 7 days after exposure to light. ERGs were recorded for the dark-adapted mice by placing an electrode in contact with the cornea and a reference electrode

through the tongue. A grounding electrode was placed intramuscularly in the hip area. The eyes were anesthetized with Localin (Fischer Pharmaceutical Labs), and dilated with tropicamide (Fischer Pharmaceutical Labs) and phenylephrine (Fischer Pharmaceutical Labs), and the corneas were kept moist with the application of carboxymethylcellulose (Fischer Pharmaceutical Labs) as needed. All procedures were performed in dim red light or darkness, and the mice were kept warm during the entire procedure. Each mouse was positioned facing the center of a Ganzfeld bowl, ensuring equal, simultaneous illumination of both eyes. ERGs were recorded inside a Faraday cage using the Espion computerized system (Diagnosys Llc, Littleton, MA). Dark-adapted ERG responses to a series of white flashes of increasing intensities (from 0.000006 to 9.6 $\text{cd} \times \text{sec}/\text{m}^2$) were recorded with inter-stimulus intervals rising from 10 s for the lowest-intensity flashes to 90 s for the highest-intensity flashes. Light adaptation was accomplished with a background illumination of 30 cd/m^2 . For analysis, the b-wave amplitude was measured from the trough of the a-wave to the peak of the b-wave, and the a-wave was measured as the difference in amplitude between the recording at 5 ms and the trough of the negative deflection.

Histological evaluation of oxidative stress and photoreceptors: Seven days after light damage, the mice were euthanized as described above, and the eyes were enucleated and cryo-sectioned at 10 μm . Anti-4 hydroxynonenal (4-HNE) antibody (10 $\mu\text{g}/\text{ml}$; Abcam (ab46545), Cambridge, UK) was used to detect oxidative stress, and anti-cleaved caspase-3 antibody (1 $\mu\text{g}/\text{ml}$, Cell Signaling Technology (#9661), Danvers, MA) was used to detect apoptosis. The immunohistochemical labeling of tissues was performed as previously described [11]. Briefly, eyes were fixed with 4% paraformaldehyde, and were placed in 30% sucrose overnight at 4 °C. Then the eyes were placed in optimal cutting temperature (OCT) solution (Scigen Scientific, Carson, CA), and placed in blocking solution (10% NGS, 0.01% Triton X in PBS) for 1 h at room temperature, followed by the addition of primary antibody overnight at 4 °C. Secondary antibody (goat anti-rabbit immunoglobulin [IgG] H&L; Alexa Fluor-488, Abcam, Cambridge, UK) was added for 1 h at room temperature. Counterstain with 4',6-diamidino-2-phenylindole (DAPI) was applied to all sections. Then, the antibody-labeled tissue sections were visualized under a fluorescent microscope using a 488 nm laser for the 4-HNE or caspase-3 antibody-labeled tissues, and a 405 nm laser for DAPI. For the evaluation of the outer nuclear layer (ONL) thickness, the sections were stained with DAPI, and the number of photoreceptor nuclei was counted at different distances from the optic nerve head (ONH).

Statistical analysis: Appropriate statistical tests were applied according to the results of a normalcy test, and the sample distribution and parameters. Biostatistical package InStat (GraphPad Software, San Diego, CA) was used for data analysis. Values over two standard deviations from the average were excluded from statistical analysis, and the mean \pm SEM is indicated. Statistical analysis was performed with one-way ANOVA, followed by the Dunnett post-test for comparison among means depending on the experimental design. For the choroidal sprouting assay and the retinal explant assay, a repeated-measure mixed-effect model (in which the random effect was the mouse) was used. An unpaired *t* test was used when only two groups were compared.

RESULTS

Modulation of the angiogenic effect of macrophages following treatment: M1 and M2a hMDMs from patients with AMD were cultured, and treated with the antioxidant supplements. The culture media was then added to the CSA cultures for 8 days, and the area of the sprouting vessel was calculated. Only treatment of M2a hMDMs with the G3 supplement was associated with a reduced sprouting area (−1.52-fold versus untreated control M2a medium, $p=0.05$, repeated-measure mixed-effect model; Figure 1B). All other treatments had no effect on the sprouting area ($p>0.05$, the repeated-measure mixed-effect model; Figure 1B). The angiogenic capacity of the M1 hMDMs was not affected by the different treatments ($p>0.05$, the repeated-measure mixed-effect model; Figure 1A). This subtype of hMDMs was found to have a stronger angiogenic effect in our previous experiments [11]. Because the antioxidants did not show an effect on this macrophage subtype, we did not conduct in vivo experiments to assess the supplement effect on neovascularization.

Modulation of the neurotoxic effect of macrophages in retinal explants: The cultured hMDMs were treated with the G1 through G4 supplements followed by coculture of the hMDMs with the mouse retinal explant. The apoptosis rate was evaluated with TUNEL labeling after 18 h of coculture. No change in the neurotoxic effect of M1 hMDMs was observed in association with the different treatments compared to the control group ($p>0.05$, Figure 2A). However, treatment with G1 was associated with an increased level of photoreceptor death compared to treatment with G2, G3, and G4 (2.13-fold, $p=0.023$, 3.96-fold, $p=0.002$ and 2.92-fold, $p=0.02$, respectively, the repeated-measure mixed-effect model, Figure 2A). Regarding the M2a hMDMs, we found that treatment with G2 and G4 was associated with an increased neurotoxic effect compared to the control group (1.37-fold, $p=0.047$ and 1.48-fold, $p=0.004$, respectively the repeated-measure

mixed-effect model), as well as compared to the G3 treatment group (1.46-fold, $p=0.01$ and 1.58-fold, $p=0.001$, respectively, the repeated-measure mixed-effect model; Figure 2B).

Effect of antioxidant treatments on photoreceptor survival in the mice model for photic retinal injury: Because the addition of antioxidant treatments modulated the deleterious effect of macrophages on photoreceptors in an in vitro model, we continued our investigation of their impact in an in vivo model which recapitulated some of the features of the atrophic stage of AMD, and where the involvement of the two subtypes of macrophages (M1 and M2a) has already been highlighted [13,31-33]. A mouse model of photic retinal injury was generated to assess the effect of antioxidant treatments on photoreceptor degeneration. Experimental conditions were optimized to obtain the loss of approximately 50% of the photoreceptor and marked retinal oxidative stress 7 days after the light exposure. Photoreceptor loss was evaluated with measurement of the ONL thickness. In addition, recruitment of myeloid cells was observed in the choroid of the light-damaged mice (Figure 3). Mice were treated with the G1 through G4 supplements with gavage during a period of 7 days before light injury and until 7 days following it. Results showed that administration of three of the four supplements (G2, G3, and G4) was associated with markedly reduced oxidative retinal injury according to 4-HNE labeling,

compared with that of untreated mice (-2.32 -fold, -2.17 -fold, and -2.18 -fold, respectively; $p<0.05$ for each of the comparisons, one-way ANOVA, Figure 4A).

We then evaluated whether the reduction of the oxidative injury level in the different groups was sufficient to allow for photoreceptor rescue in this model, using ERG, histology, and immunostaining for activated caspase 3. The immunostaining showed no difference in the number of photoreceptors positive for activated caspase 3 across the G1 through G4 treatment groups and the vehicle group ($p>0.05$, unpaired t test; Figure 4B). In accordance with those results, histological analysis showed similar ONL thickness in the G1 through G4 treatment groups compared with the vehicle group (Figure 4C), although the G2 and G4 treatment groups showed a trend toward increased damage, reinforcing the results obtained in the retinal explant assay (Figure 4D). Finally, there was an approximately 40% decrease in retinal function per ERG after light injury, in the vehicle group (-1.78 -fold versus control values, $p<0.05$, one-way ANOVA), and in the G1 (-1.85 -fold, $p<0.01$, one-way ANOVA), G2 (-1.98 -fold, $p<0.01$, one-way ANOVA), G3 (-1.74 -fold, $p<0.05$, one-way ANOVA), and G4 (-2.08 -fold, $p<0.01$, one-way ANOVA) treatment groups (Figure 4F). However, there was no difference between the ERG values of the mice treated with the G1 through G4 supplements and the vehicle group (Figure 4E,F).

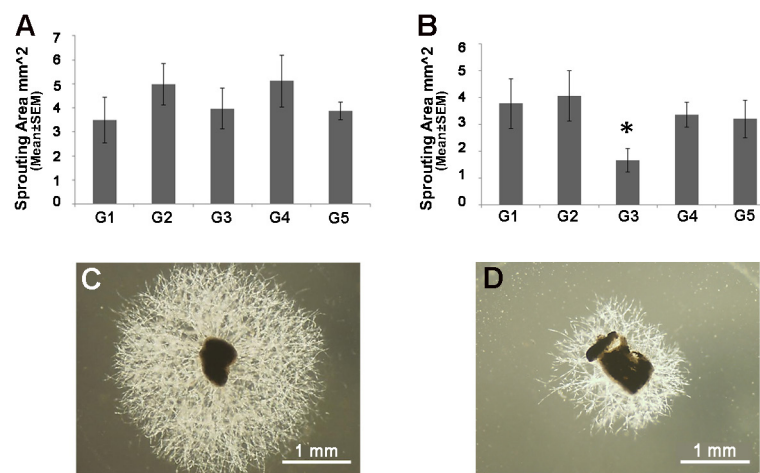


Figure 1. In vitro assessment of the effect of antioxidant supplements on the angiogenic properties of M1 and M2a hMDMs. Four antioxidant treatments (G1–G4; see the details in the Methods section) were added to the culture medium of M1 ($n=7$) and M2a ($n=8$) human monocyte-derived macrophages (hMDMs). The addition of untreated culture medium served as control (G5). Choroid tissue was cultured for 8 days with the supernatants from M1 (A) and M2a (B) hMDMs treated with the different supplements. The sprouting area was calculated using ImageJ software (repeated-measure mixed-effect model, $*p\leq 0.05$). C: Representative image from control is shown. D: The G3-treated medium culture of M2a macrophages is shown.

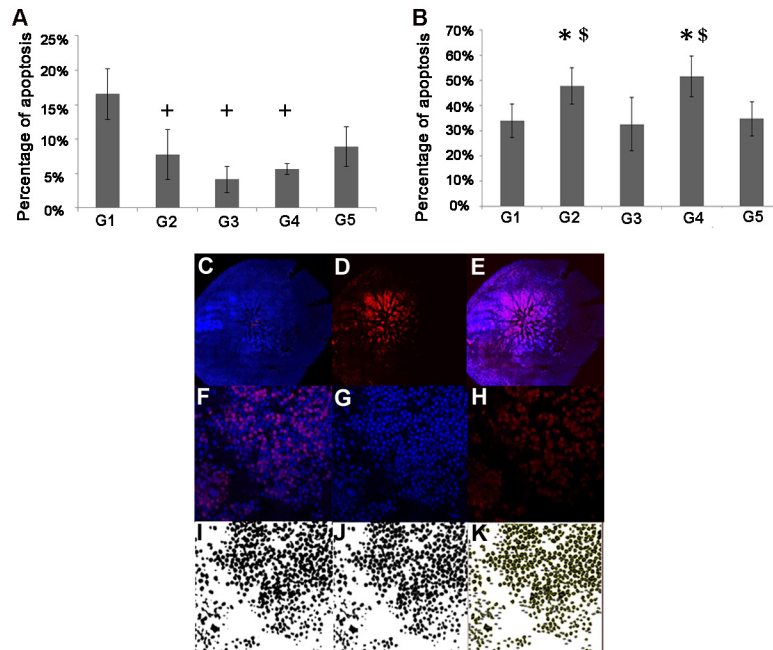


Figure 2. Ex vivo assessment of the effect of antioxidant treatments on hMDM neurotoxicity. Mouse retinal explants were incubated for 18 h with M1 (A, n=7) or M2a (B, n=8) human monocyte-derived macrophages (hMDMs) which were supplemented with the four antioxidant treatments (G1–G4). Un-supplemented media served as control (G5). The apoptosis level was evaluated using terminal deoxynucleotidyl transferase dUTP nick end labeling (TUNEL) labeling under a confocal microscope. No treatments affected the toxicity level of the M1 hMDMs compared to that of the control group. However, treatment with G2, G3, and G4 reduced the toxicity of the M1 hMDMs compared to treatment with G1 (repeated-measure mixed-effect model, $^+p \leq 0.05$ compared to G1 (A)). The M2a hMDMs supplemented with the G2 and G4 treatments were associated with an increasing toxicity level compared to that of the control group and the G3 treatment group ($^*p \leq 0.05$ compared with control and $^{\$}p \leq 0.05$ compared to G3 (B)). For apoptosis quantification, the entire retina was stained with 4',6-diamidino-2-phenylindole (DAPI)-nuclei labeling (blue; C) and TUNEL labeling (red; D), and then merged (E). Eleven fields were automatically chosen around the optic nerve, magnified at 40X (F). Photos from each field were split into blue and red channels (G, H), and then converted into 8-bit images (I), which underwent water sheet processing to delineate each cell (J). The total numbers of cells were then automatically quantified, and the numbers of apoptotic cells were calculated as the percentage of the total number of cells stained with DAPI (K).

DISCUSSION

We previously showed that antioxidant formulas may regulate the expression profile of hMDMs, thus potentially modulating their proinflammatory and pro-oxidative phenotype [19]. In the present work, we showed that such formulas may modulate the angiogenic and cytotoxic effects of hMDMs ex vivo. Furthermore, antioxidant treatments were associated with milder oxidative retinal injury in the photic injury model. These effects were evident after treatment with a combination of lycopene and carnosic acid in addition to lutein and zeaxanthin and zinc. This combination (G3 formula) reduced the angiogenic and cytotoxic effects of the treated M2a polarized hMDMs ex vivo. Interestingly, the same combination of supplements had previously showed a strong impact on the expression of several genes, including antioxidant genes, proangiogenic genes, and proinflammatory genes, as well as an important effect on ROS generation in polarized macrophage cultures [19].

Ex vivo neurotoxic assay revealed that M2a hMDMs are more deleterious than M1 hMDMs (approximately 35% versus less than 10%, respectively), suggesting the implication of M2a macrophages more than that of M1 macrophages in the atrophic stage of AMD where the death of retinal cells occurs. In addition, we showed that treatment with lutein and zeaxanthin, and zinc (the G2 formula) increased the neurotoxic effect of M2a hMDMs, as well as exacerbated the ROS secretion from this same subtype of macrophages [19]. Finally, the same formula showed a trend to increase the loss of ONL thickness in vivo. Until today, oral supplementation with the AREDS or AREDS2 formulations (antioxidant vitamins C and E, lutein, zeaxanthin, and zinc) is the only treatment administered to patients with AMD at the atrophic stage of the disease. Taken together, these results could provide a potential explanation why the AREDS formulation fails to slow the progression of aAMD.

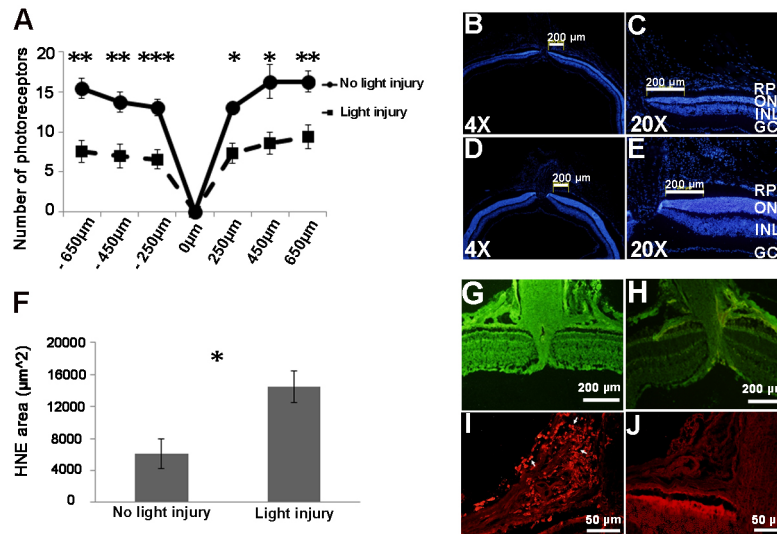


Figure 3. Establishing the model of photic retinal injury. Exposure of BALB/c mice to bright light of 8000 lux intensity for 3 h led to 50% loss of photoreceptors 7 days after light injury at different distances from the optic disc (–2-fold, unpaired t test, * $p=0.01$, ** $p=0.003$, *** $p=0.0003$, A: Histological sections, stained with 4',6-diamidino-2-phenylindole (DAPI; blue signal), showed reduction of the ONL thickness after photic injury (B and C) compared to that of the control group (D and E). An increase in the oxidative stress level was observed 7 days after the light injury (1.63-fold, unpaired t test, * $p=0.009$, F and G), compared to the control mice not exposed to light (H), as shown with the 4-hydroxynonenal (4-HNE) antibody label tissues (green signal). The fluorescence intensity of the 4-HNE antibody label tissue was measured using ImageJ software, and the negative control of 4-HNE antibody label tissue value was subtracted. Recruitment of cd11b+ cells (red signal, arrows) was observed 7 days after light injury (I), compared to the control group (J). GCL, ganglion cell layer; INL, inner nuclear layer; ONL, outer nuclear layer.

Albeit a comprehensive view of the mechanism of the development of AMD is still lacking, several recent studies highlighted the role of immune cells in the progression of AMD [34-36], and others suggested that oxidative injury constitutes an important factor in the progression of the disease [37]. It is also known that macrophages may exert oxidative injury [19]. Thus, modulating the macrophage phenotype to reduce their oxidative stress properties in the retina could potentially represent a therapeutic strategy for AMD.

Modulation of macrophage secretion, and actions by carotenoid and phenolic components, has previously been shown. For example, lutein has been demonstrated to suppress macrophage recruitment and MCP-1 (CCL2) expression in the photo-stressed RPE-choroid [38]. Similarly, lycopene and carnosic acid have been found to modulate macrophage function in a model of acute peritonitis [39]. In accordance with those results, we showed that a supplement mixture that also includes lutein, lycopene, and carnosic acid, and zinc could specifically change the properties of hMDMs from patients with AMD, in ex vivo models for angiogenesis and cytotoxicity that are relevant for aAMD and nvAMD, respectively.

The effects of lutein and carnosic acid were previously tested in a model of photic retinal injury [40]. Mice that

received a diet containing 0.1% lutein, equivalent to 170 mg/kg bodyweight per day, showed a decrease in photoreceptor loss. Another study suggested a protective effect of intraperitoneal injection of carnosic acid against photoreceptor death triggered by light injury [41]. Other studies evaluated the protective effect of lycopene and beta-carotene against oxidative damage in HT29 cells at different concentrations, and found that only low dosages have a beneficial effect on retinal oxidative injury, but that this protective effect is rapidly lost at higher doses [42]. In contrast with these previous studies, the four formulas tested in this study had an impact on the retinal oxidative stress level, but did not have an effect on photoreceptor loss. A possible explanation for the varying effect of the formulas across the studies could be that the dosage used in the present study is twofold lower than those administered in the first study cited above. The mean level of lutein consumption from foods is estimated at less than 2 mg/day, suggesting that the doses used in the reviewed trial were 85-fold higher than what is typically consumed in the diet, and 8.5-fold higher than the observed safe level (OSL) [43]. In addition, the method with which we administered the lutein compound differed from that in those studies.

The present study has several potential limitations, including that only one supplement dosage for each formula

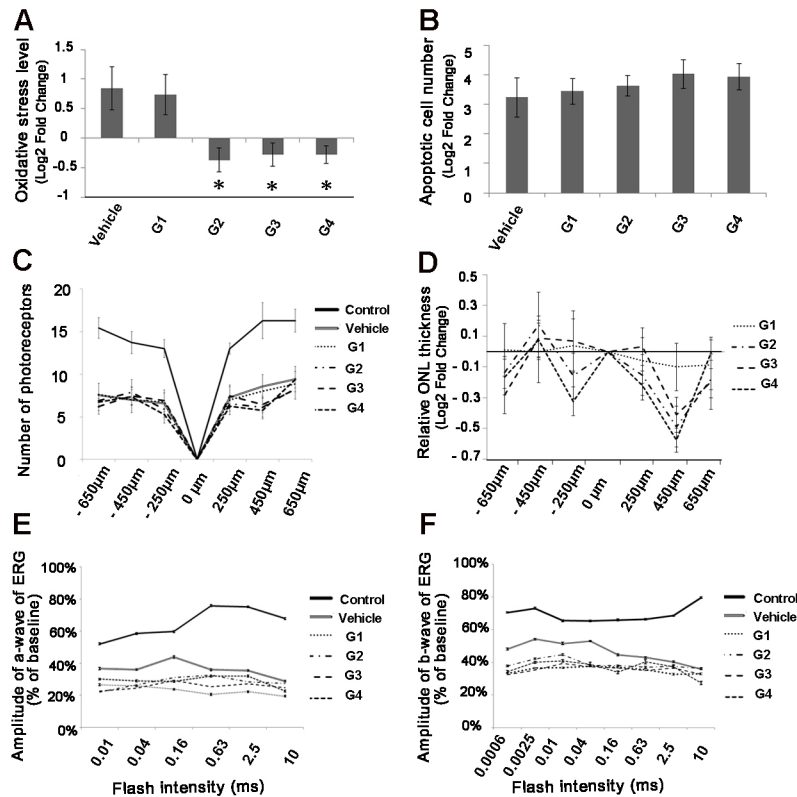


Figure 4. Assessment of the effect of antioxidant treatment on photic retinal injury in mice. Mice treated with the G2, G3, and G4 formulas (see the Methods section for details) were evaluated for oxidative injury (A), apoptosis (B), outer nuclear layer thickness (C, D), and electroretinography (ERG) response (E, F). Oxidative injury was evaluated with measurement of 4-hydroxynonenal (4-HNE) antibody label tissue. A reduced level of HNE antibody label tissue was detected 7 days after the exposure to light, compared to the vehicle-treated group ($n=8$, one-way ANOVA Dunnett, $*p \leq 0.05$, A). Apoptosis was assessed with measurement of the number of activated caspase 3⁺ cells, which was similar across the treatment and vehicle groups (one-way ANOVA, $p > 0.05$, B). The level of oxidative stress and the number of caspase 3⁺ cells were normalized to the control group (not exposed to light). None of the treatments conferred a protective effect on the photoreceptors, as shown with the measurements of the number of nuclei in the outer nuclear layer (one-way ANOVA, $p > 0.05$, C and D), and with ERG recording (one-way ANOVA, $p > 0.05$, E and F). The measurement of ONL thickness was normalized to the vehicle group.

was tested, and a single *in vivo* model was used. However, the findings were consistent with our previous study on the effect of the same formulas on gene and protein expression in hMDMs [19]. We also did not test the effect of the formulas on choroidal neovascularization *in vivo*. This evaluation was not performed, because *ex vivo* studies suggested that the supplements modulate M2a, but not M1 hMDMs. In our previous study, M1 hMDMs from patients with AMD showed a stronger proangiogenic effect compared with M2a hMDMs, and thus, should provide a more important therapeutic target in that respect [11].

In conclusion, this study revealed that a supplements mixture containing lutein + zeaxanthin, zinc, lycopene, and carnosic acid modulates the angiogenic and neurotoxic actions of M2a hMDMs *in vitro*. In addition, we showed that albeit antioxidant treatments reduce the level of oxidative stress considerably in the light-damaged retina, they did not

prevent photoreceptor degeneration in this acute model of retinal injury. The model of light damage is relatively aggressive, and promotes damage over the course of a week, and it is still possible that such supplements would demonstrate protective damage in the slower degeneration that is common in AMD. Future research should be conducted to explore this possibility.

ACKNOWLEDGMENTS

The research was supported by a generous research grant from Hadassah-France. Experimental protocols and for the study involving human subjects were approved by the local committee on Research Involving Human Subjects of the Hadassah Medical Center (File #22-03.08.07). All patients and controls signed informed consent forms that adhered to the tenets of the Declaration of Helsinki before participating

in the study. Ethical approval for all protocols involving animals were obtained by the Authority for Biologic and Biomedical Models (ABBM) and the University Ethics Committee for the Care and Use of Laboratory Animals in Hebrew University, which is certified by the Association for Assessment and Accreditation of Laboratory Animal Care (AAALAC; ethical approval number: MD-15-14240-4, NIH approval number: OPRR-A01-5011). All researchers working with laboratory animals underwent approval by the ethics committee of the ABBM to allow them to ethically work with laboratory animals. All guidelines with regards to human and ethical treatment of laboratory animals (from ARVO) were followed.

REFERENCES

- Sarks SH, Van Driel D, Maxwell L, Killingsworth M. Softening of drusen and subretinal neovascularization. *Trans Ophthalmol Soc U K* 1980; 100:414-22. [PMID: 6171074].
- Penfold P, Killingsworth M, Sarks S. An ultrastructural study of the role of leucocytes and fibroblasts in the breakdown of Bruch's membrane. *Aust J Ophthalmol* 1984; 12:23-31. [PMID: 6732655].
- Jonas JB, Tao Y, Neumaier M, Findeisen P. Monocyte chemoattractant protein 1, intercellular adhesion molecule 1, and vascular cell adhesion molecule 1 in exudative age-related macular degeneration. *Arch Ophthalmol* 2010; 128:1281-6. [PMID: 20937997].
- Grunin M, Burstyn-Cohen T, Hagbi-Levi S, Peled A, Chowers I. Chemokine receptor expression in peripheral blood monocytes from patients with neovascular age-related macular degeneration. *Invest Ophthalmol Vis Sci* [Internet]. 2012/07/14 ed. 2012;53(9):5292-300.
- Mantovani A, Sozzani S, Locati M, Allavena P, Sica A. Macrophage polarization: tumor-associated macrophages as a paradigm for polarized M2 mononuclear phagocytes. *Trends Immunol* 2002; 23:549-55. [PMID: 12401408].
- Martinez FO, Sica A, Mantovani A, Locati M. Macrophage activation and polarization. *Front Biosci* 2008; 13:453-61. [PMID: 17981560].
- Mantovani A, Sica A, Sozzani S, Allavena P, Vecchi A, Locati M. The chemokine system in diverse forms of macrophage activation and polarization. *Trends Immunol* 2004; 25:677-86. [PMID: 15530839].
- Sica A, Invernizzi P, Mantovani A. Macrophage plasticity and polarization in liver homeostasis and pathology. *Hepatology* 2014; 59:2034-42. [PMID: 24115204].
- Martinez FO, Gordon S. The M1 and M2 paradigm of macrophage activation: time for reassessment. *F1000Prime Rep* [Internet]. 2014/03/29 ed. 2014;6(March):13.
- Mills CD. M1 and M2 Macrophages: Oracles of Health and Disease. *Crit Rev Immunol* 2012; 32:463-88. [PMID: 23428224].
- Hagbi-Levi S, Grunin M, Jaouni T, Tiosano L, Rinsky B, Elbaz-Hayoun S, Peled ACI, Hagbi-Levi S, Grunin M, Jaouni T, Tiosano L, Rinsky B, Elbaz-Hayoun S, Peled A, Chowers I. Pro-Angiogenic Characteristics of Activated Macrophages from Patients with Age-related Macular Degeneration. *Neurobiol Aging* [Internet]. 2016 Dec [cited 2016 Dec 28];51:71-82.
- Sennlaub F, Auvynet C, Calippe B, Lavalette S, Poupel L, Hu SJ, Dominguez E, Camelo S, Levy O, Guyon E, Saederup N, Charo IF, Van Rooijen N, Nandrot E, Bourges J-LL, Behar-Cohen F, Sahel J-AA, Guillonneau X, Raoul W, Combadiere C. CCR2(+) monocytes infiltrate atrophic lesions in age-related macular disease and mediate photoreceptor degeneration in experimental subretinal inflammation in Cx3cr1 deficient mice. *EMBO Mol Med* 2013; 5:1775-93. [PMID: 24142887].
- Cruz-Guilloty F, Saeed AM, Echegaray JJ, Duffort S, Ballmick A, Tan Y, Betancourt M, Viteri E, Ramkhellawan GC, Ewald E, Feuer W, Huang D, Wen R, Hong L, Wang H, Laird JM, Sene A, Apte RS, Salomon RG, Hollyfield JG, Perez VL. Infiltration of proinflammatory m1 macrophages into the outer retina precedes damage in a mouse model of age-related macular degeneration. *Int J Inflam* [Internet]. 2013;2013:503725.
- Ambati J, Fowler BJ. Mechanisms of age-related macular degeneration. *Neuron* [Internet]. 2012/07/17 ed. 2012;75(1):26-39.
- Cai J, Nelson KC, Wu M, Sternberg P Jr, Jones DP. Oxidative damage and protection of the RPE. *Prog Retin Eye Res* 2000; 19:205-21. [PMID: 10674708].
- Beatty S, Koh H-H, Phil M, Henson D, Boulton M. The role of oxidative stress in the pathogenesis of age-related macular degeneration. *Surv Ophthalmol* 2000; 45:115-34. [PMID: 11033038].
- Khandhadia S, Lotery A. Oxidation and age-related macular degeneration: insights from molecular biology. *Expert Rev Mol Med* [Internet]. 2010;12(October 2010):e34.
- Age-Related Eye Disease Study 2 Research G. Chew EY, Clemons TE, Sangiovanni JP, Danis RP, Ferris 3rd FL, Elman MJ, Antoszyk AN, Ruby AJ, Orth D, Bressler SB, Fish GE, Hubbard GB, Klein ML, Chandra SR, Blodi BA, Domalpally A, Friberg T, Wong WT, Rosenfeld PJ, Agron E, Toth CA, Bernstein PS, Sperduto RD. Secondary analyses of the effects of lutein/zeaxanthin on age-related macular degeneration progression: AREDS2 report No. 3. *JAMA Ophthalmol* 2014; 132:142-9. [PMID: 24310343].
- Rinsky B, Hagbi-Levi S, Elbaz-Hayoun S, Grunin M, Chowers I. Characterizing the effect of supplements on the phenotype of cultured macrophages from patients with age-related macular degeneration. *Mol Vis* 2017; 23:889-899-[PMID: 29259394].
- Collins TJ. ImageJ for microscopy. *Biotechniques* 2007; 43:25-30. [PMID: 17936939].
- Bouhlef MA, Derudas B, Rigamonti E, Dièvert R, Brozek J, Haulon S, Zawadzki C, Jude B, Torpier G, Marx N, Staels

- B, Chinetti-Gbaguidi G. PPAR γ Activation Primes Human Monocytes into Alternative M2 Macrophages with Anti-inflammatory Properties. *Cell Metab* 2007; 6:137-43. [PMID: 17681149].
22. Gelinas L, Falkenham A, Oxner A, Sopol M, Legare JF. Highly purified human peripheral blood monocytes produce IL-6 but not TNF α in response to angiotensin II. *J Renin Angiotensin Aldosterone Syst* 2011; 12:295-303. [PMID: 21393356].
 23. Martinez FO. The transcriptome of human monocyte subsets begins to emerge. *J Biol* 2009; 8:99-[PMID: 20067595].
 24. Pelegrin P, Surprenant A. Dynamics of macrophage polarization reveal new mechanism to inhibit IL-1 β release through pyrophosphates. *EMBO J* [Internet]. 2009/06/19 ed. 2009;28(14):2114–27.
 25. Allavena P, Piemonti L, Longoni D, Bernasconi S, Stoppacciaro A, Ruco L, Mantovani A. IL-10 prevents the differentiation of monocytes to dendritic cells but promotes their maturation to macrophages. *Eur J Immunol* 1998; 28:359-69. [PMID: 9485215].
 26. Shao Z, Friedlander M, Hurst CG, Cui Z, Pei DT, Evans LP, Juan AM, Tahiri H, Duhamel F, Chen J, Sapieha P, Chemtob S, Joyal J-SS, Smith LEH, Tahir H, Duhamel F, Chen J, Sapieha P, Chemtob S, Joyal J-SS, Smith LEH. Choroid sprouting assay: an ex vivo model of microvascular angiogenesis. *PLoS One* [Internet]. 2013/08/08 ed. 2013;8(7):e69552.
 27. Wenzel A, Grimm C, Samardzija M, Remé CE. The genetic modifier Rpe65^{Leu450}: Effect on light damage susceptibility in c-Fos-deficient mice. *Invest Ophthalmol Vis Sci* 2003; 44:2798-802. [PMID: 12766089].
 28. Mattapallil MJ, Wawrousek EF, Chan CC, Zhao H, Roychoudhury J, Ferguson TA, Caspi RR. The Rd8 mutation of the Crbl gene is present in vendor lines of C57BL/6N mice and embryonic stem cells, and confounds ocular induced mutant phenotypes. *Invest Ophthalmol Vis Sci* [Internet]. 2012/03/27 ed. 2012;53(6):2921–7.
 29. Chang B, Hurd R, Wang J, Nishina P. Survey of Common Eye Diseases in Laboratory Mouse Strains. *Invest Ophthalmol Vis Sci* 2013; 54:4974-81. [PMID: 23800770].
 30. Grimm C, Reme CE, Remé CE. Light damage as a model of retinal degeneration. *Methods Mol Biol* 2013; 935:87-97. [PMID: 23150362].
 31. Jiao H, Natoli R, Valter K, Provis JM, Rutar M. Spatiotemporal cadence of macrophage polarisation in a model of light-induced retinal degeneration. *PLoS One* 2015; 10:e0143952-Internet[PMID: 26630454].
 32. Ni YQ, Xu GZ, Hu WZ, Shi L, Qin YW, Da CD. Neuroprotective effects of naloxone against light-induced photoreceptor degeneration through inhibiting retinal microglial activation. *Invest Ophthalmol Vis Sci* [Internet]. 2008/06/03 ed. 2008;49(6):2589–98.
 33. Zhang M, Xu G, Liu W, Ni Y, Zhou W. Role of fractalkine/CX3CR1 interaction in light-induced photoreceptor degeneration through regulating retinal microglial activation and migration. *PLoS One* [Internet]. 2012/04/27 ed. 2012;7(4):e35446.
 34. Patel M, Chan CC. Immunopathological aspects of age-related macular degeneration. *Semin Immunopathol* 2008; 30:Internet[PMID: 18299834].
 35. Penfold PL, Madigan MC, Gillies MC, Provis JM. Immunological and aetiological aspects of macular degeneration. *Prog Retin Eye Res* [Internet]. 2001/04/05 ed. 2001;20(3):385–414.
 36. Kaarniranta K, Salminen A. Age-related macular degeneration: activation of innate immunity system via pattern recognition receptors. *J Mol Med* [Internet]. 2008/11/15 ed. 2009;87(2):117–23.
 37. Winkler BS, Boulton ME, Gottsch JD, Sternberg P. Oxidative damage and age-related macular degeneration. *Mol Vis* 1999; 5:32-[PMID: 10562656].
 38. Kamoshita M, Toda E, Osada H, Narimatsu T, Kobayashi S, Tsubota K, Ozawa Y. Lutein acts via multiple antioxidant pathways in the photo-stressed retina. *Sci Rep* 2016; 6:30226-[PMID: 27444056].
 39. Hadad N, Levy R. The synergistic anti-inflammatory effects of lycopene, lutein??-carotene, and carnosic acid combinations via redox-based inhibition of NF-??B signaling. Vol. 53 *Free Radic Biol Med* 2012; 53:1381-91. [PMID: 22889596].
 40. Sasaki M, Yuki K, Kurihara T, Miyake S, Noda K, Kobayashi S, Ishida S, Tsubota K, Ozawa Y. Biological role of lutein in the light-induced retinal degeneration. *J Nutr Biochem* 2012; 23:423-9. [PMID: 21658930].
 41. Rezaie T, McKercher SR, Kosaka K, Seki M, Wheeler L, Viswanath V, Chun T, Joshi R, Valencia M, Sasaki S, Tozawa T, Satoh T, Lipton S a. Protective effect of carnosic acid, a pro-electrophilic compound, in models of oxidative stress and light-induced retinal degeneration. *Invest Ophthalmol Vis Sci* 2012; 53:7847-54. [PMID: 23081978].
 42. Lowe GM, Booth L a, Young a J, Bilton RF. Lycopene and beta-carotene protect against oxidative damage in HT29 cells at low concentrations but rapidly lose this capacity at higher doses. *Free Radic Res* 1999; 30:141-51. [PMID: 10193582].
 43. Shao A, Hathcock JN. Risk assessment for the carotenoids lutein and lycopene. *Regul Toxicol Pharmacol* 2006; 45:289-98. [PMID: 16814439].
 44. Age-Related Eye Disease Study (AREDS) design implications. AREDS report number 1. *Control Clin Trials* 1999; 20:573-600. .

Articles are provided courtesy of Emory University and the Zhongshan Ophthalmic Center, Sun Yat-sen University, P.R. China. The print version of this article was created on 5 September 2019. This reflects all typographical corrections and errata to the article through that date. Details of any changes may be found in the online version of the article.